

Continuum Models and Discrete Systems CMDS 11

Proceedings of the International Symposium held in Paris
July 30th–August 3rd 2007

Dominique Jeulin, Samuel Forest, Editors



Collection Sciences de la matière

Dans la même collection

François Delamare

Bleus en poudre

De l'Art à l'Industrie 5000 ans d'innovatio

Bernard Jaoul

Etude de la plasticité et application aux métaux

Besson, D. Moinereau, D. Steglich

EUROMECH - MECAMAT 2006

9th European Mechanics of Materials Conference Local Approach to Fracture

Samuel Forest

Milieux continus généralisés et matériaux hétérogènes

C. Berdin, J. Besson, S. Bugat, R. Desmorat, F. Feyel, S. Forest, E. Lorentz, E. Maire,

T. Pardoën, A. Pineau et B. Tanguy

under the supervision of Jacques Besson _

Local approach to fracture

Oeuvre collectif coordonné par Eric Felder

Surfaces, tribologie et formage des matériaux

Sous la direction de : Alain Thorel, Jacques Masounave et Michel Suéry

Intérêts technologiques et marchés potentiels des composites à matrice métallique

André Rousset

Gargamelle et les courants neutres

Témoignage d'une découverte scientifique

Coordonnateurs : J.L. Chenot et F. Delamare

La mise en forme des matériaux

Vingt ans de recherche au Cemef



© École des mines de Paris, 2008
60, boulevard Saint-Michel - 75272 Paris Cedex 06 - France
email : presses@ensmp.fr
<http://www.ensmp.fr/Presses>

© **Photo de couverture** : D. Jeulin

© **Photo 4^e de couverture** : M. Filoche, B. Sapoval, F. Willot, Y.P. Pellegrini

Samuel Forest

ISBN : 978-2-35671-000-0

Dépôt légal : 2008

Achevé d'imprimer en 2008 (Paris)

Tous droits de reproduction, de traduction, d'adaptation et d'exécution réservés pour tous les pays.

Contents

Preface	11
I Thermodynamics, transport theory and statistical mechanics in the context of continuum modeling of discrete systems	13
GL: Duality and phase diagram of one dimensional transport <i>S.M. Bhattacharjee</i>	15
On entropy of microstructure and secondary thermodynamics <i>V. Berdichevsky</i>	25
The self-consistent effective medium approximation: new types of critical points in a composite medium <i>D.J. Bergman, R. Magier</i>	29
A theory of mixtures for heterogeneous solids and its application to spinodal decomposition and coarsening <i>T. Böhme, W. H. Müller</i>	37
II Continuum mechanics of complex fluids with microstructure	45
Turbulence in porous media & scaling behavior of fractured surfaces: A conjecture <i>B.K. Chakrabarti</i>	47
Long-range hydrodynamic response of complex liquids <i>H. Diamant</i>	51
Modeling film flow of complex fluids, a review <i>P. Manneville</i>	57
The Cahn-Hilliard equation with constant and degenerate mobilities <i>A. Novick-Cohen</i>	63
Features of immiscible steady-state two-phase flow in porous Media <i>T. Ramstad, A. Hansen</i>	69

Transient evaporation of drops on an heterogeneous surface <i>J. Frassy, C. Lecot, A. Soucemarianadin</i>	71
Thermodynamic properties of imperfect solids near freezing point <i>S. P. Singh, S. P. Das</i>	79
A continuum model with microstructure for liquids with vapour bubbles <i>M. Bongué Boma, M. Brocato</i>	87
GL: Discrete network approximation for highly packed particle filled composites <i>L. Berlyand</i>	93
III Continuum mechanics of deformable solids with microstructure	95
GL: On modifications of Newton's second law and linear continuum elastodynamics <i>G.W. Milton</i>	97
Balance laws in micromorphic elasticity <i>M. Lazar, C. Anastassiadis</i>	99
The micromorphic approach to plasticity and diffusion <i>S. Forest</i>	105
Instability and energy minimization in solids: formation of microstructures <i>H. Petryk</i>	113
Periodic homogenization of Hamilton-Jacobi-Bellman equations <i>N. Ichihara</i>	119
Effective properties of matrix composites with nonellipsoidal inclusions <i>S. Kanaun, S. Babaii Kochecksaraii</i>	125
Influence of external stresses and pore pressure on deformation of crack-like inhomogeneities in a poroelastic medium <i>V. M. Levin, J.M. Alvarez-Tostado</i>	131
Convergence analysis of the Bül-Reese discrete model for rubber <i>R. Alicandro, M. Cicalese, A. Gloria</i>	137
Homogenization-based constitutive models for two-dimensional viscoplastic porous media with evolving microstructure <i>K. Danas, M.I. Idiart, P. Ponte Castañeda</i>	143
Potential influence of microstructural morphology on the viscoplastic flow of two-phase polycrystals <i>N. Rupin, M. Bornert, P. Gilormini, A. Zaoui, C. Pinna</i>	149
A buckling problem for graphene sheets <i>J. Galagher, Y. Milman, S. Ryan, D. Golovaty, P. Wilber, A. Buldum</i>	155

Viscoplastic phase field modelling of rafting in Ni base superalloys	
<i>A. Gaubert, A. Finel, Y. Le Bouar, G. Boussinot</i>	161
On the geodesic property of strain field patterns in elasto-plastic composites	
<i>D. Jeulin, W. Li, M. Ostoja-Starzewski</i>	167
On the lattice dynamics of a fractal gasket	
<i>T. M. Michelitsch, S. Derogar, A. F. Nowakowski, F.C.G.A. Nicolleau</i>	173
Towards continuum mechanics of fractal materials	
<i>M. Ostoja-Starzewski</i>	179
On a statistical theory of critical events in microstructural evolution	
<i>K. Barmak, M. Emelianenko, D. Golovaty, D. Kinderlehrer, S. Ta'asan</i>	185
IV Fundamentals of fracture, defect dynamics, fatigue, and fracture dynamics on different microlevels	195
GL: Statistics of brittle cleavage fracture in steels	
<i>A. Pineau</i>	197
GL: A physically based constitutive model for FCC metals with applications to dynamic hardness	
<i>G. Voyiadjis, A. Almasri, A. N. Palazotto</i>	213
Scaling properties of fracture surfaces	
<i>D. Bonamy, L. Ponson, C. Guerra, E. Bouchaud, L. Barbier, H. Auradou, J.P. Hulin</i>	223
Solution asymptotics near maximum friction surfaces in plane strain block compression: various viscoplastic laws with a saturation stress	
<i>G. Mishuris, W. Miszuris, S. Alexandrov</i>	225
GL: Delamination of a bi-material strip by a steady-state interfacial crack	
<i>N.V. Movchan, G. Mishuris</i>	231
Best column. An historical problem of Leonhard Euler.	
<i>M. Sauvageot, J.I. Diaz</i>	243
Dynamics of breakdown in the RRTN model for nonlinear complex systems	
<i>A.K. Sen, S. Mozumdar</i>	251
V Dislocations and plasticity	257
Depinning and motion of crystal dislocations	
<i>L.L. Bonilla, A. Carpio</i>	259
Homogeneous nucleation of dislocations	
<i>A. Carpio, I. Plans, L.L. Bonilla</i>	265

On the range of 3D dislocation pair correlations <i>F. F. Csikor, I. Groma, T. Hochrainer, D. Weygand, M. Zaiser</i>	271
Peierls-Nabarro Galerkin approach to instationary dislocation motion and interaction <i>C. Denoual, Y.P. Pellegrini, L. Pillon</i>	277
Nanoindentation through the scales: from the atomic to continuum plasticity <i>M. Fivel, H.-J. Chang, D. Rodney, M. Verdier, K.H. Oh</i>	279
From discrete dislocation dynamics to a phase field theory of dislocations <i>I. Groma, G. Györgyi</i>	285
Introducing dislocation climb in discrete dislocation dynamics <i>D. Mordehai, E. Clouet, M. Fivel, M. Verdier</i>	291
“Plasticity” in silica via molecular dynamics simulations <i>C. L. Rountree, M. Talamali, D. Bonamy, D. Vandembroucq, S. Roux, E. Bouchaud</i>	297
Continuum theory of evolving dislocation fields and plastic deformation <i>R. Sedláček, C. Schwarz, J. Kratochvíl, E. Werner</i>	299
 VI New developments in continuum theory; non classical models, and discrete vs. continuum models	 305
GL: Waves and filtering in periodic thin-walled structures with cracks <i>V.V. Zalipaev, I.S. Jones, A.B. Movchan</i>	307
Discrete modelling for entangled materials near percolation thresholds <i>C. Barbier, F. Dalmas, R. Dendievel, D. Rodney</i>	319
Interpenetrating phase composites: micromechanical analysis of damage behavior <i>L. Mishnaevsky Jr</i>	325
 VII Granular materials: statics and dynamics	 331
GL: Coarse graining in granular gases and solids <i>I. Goldhirsch, C. Goldenberg</i>	333
Particle displacements in the elastic deformation of amorphous materials: local fluctuations versus non-affine field <i>C. Goldenberg, A. Tanguy, J.-L. Barrat</i>	345
Multifield continuum modelling for materials with lattice microstructure <i>P. Trovalusci, V. Sansalone</i>	351

VIII	Continuum theory of living structures	357
	GL: Applications of a theory of sequence-dependent DNA elasticity that accounts for intramolecular electrostatic forces <i>Y.Y. Biton and B.D. Coleman</i>	359
	Biofluidmechanics of reproduction <i>L. Fauci</i>	383
	The human respiratory airway system: a robust transport system <i>M. Filoche, B. Sapoval</i>	385
IX	Composite media and meta-materials	391
	GL: Dynamic mass density and acoustic metamaterials <i>P. Sheng, J. Mei, Z. Liu, W. Wen</i>	393
	Exact results for the macroscopic conductivity tensor of a two-constituent composite with a 2D columnar microstructure <i>D.J. Bergman, X. Li, Y.M. Strelniker</i>	413
	On grain size dispersion effects in metallic polycrystals and internal lengths associated with discrete plastic slip heterogeneities <i>S. Berbenni, N. Nicaise, T. Richeton, M. Berveiller</i>	417
	From 3D imaging of structures to diffusive properties of anisotropic cellular materials <i>E. Brun, J. Vicente, F. Topin, R. Ocelli</i>	423
	Statistical representative volume element for predicting the dielectric permittivity of random media <i>D. Jeulin, M. Moreaud</i>	429
	Piezoelectric effect in composites with different poling directions constituents <i>E. López-López, F.J. Sabina, R. Guinovart-Díaz, J. Bravo-Castillero, R. Rodríguez-Ramos</i>	437
	Fast Fourier Transform computations and build-up of plastic deformation in 2D, elastic-perfectly plastic, pixelwise disordered porous media <i>F. Willot, Y.-P. Pellegrini</i>	443
	Representative volume element size for random elastic composites: the correlation function method <i>K. Sab, B. Nedjar</i>	451
	List of Participants	457
	Index	461

Preface

The 11th International Symposium on Continuum Models and Discrete Systems CMDS 11 took place in Ecole des Mines de Paris (July 30th August 3rd 2007). Previous CMDS Symposia were organised in Kielce (Poland, 1975), Mont Gabriel (Canada, 1977), Freudenstadt (Federal Republic of Germany, 1979), Stockholm (Sweden, 1981), Nottingham (United Kingdom, 1985), Dijon (France, 1989), Paderborn (Germany, 1992), Varna (Bulgaria, 1995), Istanbul (Turkey, 1998) and Shoshon (Israel, 2003). The broad interdisciplinary character, the limited number of participants (not exceeding 100) and the unofficial and friendly atmosphere, made these meetings well-acknowledged places of highly fruitful contacts and exchange of ideas, methods and results.

The spirit of CMDS meetings is to stimulate an extensive and active interdisciplinary research. Attendance of speakers was made possible thanks to invitations by the International Scientific Committee, composed as follows:

David Bergman (Chairman CMDS 10), Tel Aviv University, Israel
Leonid Berlyand, Pennsylvania State University, USA
Elisabeth Bouchaud, CEA, Saclay, France
B. K. Chakrabarty, Saha institute of Nuclear Physics, Calcutta, India
Samuel Forest, Ecole des Mines de Paris, France
Hans Jürgen Herrmann, Stuttgart University, Germany
Esin Inan (Chairwoman CMDS 9), Istanbul Technical University, Turkey
Dominique Jeulin (Chairman CMDS 11), Ecole des Mines de Paris, France
Mark Kachanov, Tufts University, USA
David Kinderlehrer, Carnegie Mellon University, USA
Valery Levin, IMP, Mexico, Mexico
G rard Maugin, Paris 6 University, France
Leon Mishnaevsky, Riso National Laboratory, Denmark
Graeme Milton, Utah University, USA
N. Movchan, University of Liverpool, UK
Martin Ostoja-Starzewski, University of Illinois at Urbana-Champaign, U.S.A.
Amy Novick-Cohen, Technion, Israel

The scientific program consisted of General Lectures (GL) and Research Communications. The ten General Lectures (45 min + 5min) introduced the most recent ideas and advances in the covered fields. The 53 Research Communications reported on important new results and methods in these fields, and were presented either in oral (20 min + 5min) or in a poster form.

The CMDS 11 Symposium was able to gather 66 scientists from 14 countries active in various areas (physics, mechanics, materials sciences, applied mathematics, engineering sciences), working on properties and applications of physical systems, where the interaction between a discrete and a continuous descrip-

tion plays a major role. These Proceedings collect the content of most lectures given at CMDS 11, and covering the following topics: statistical mechanics, mechanics of complex fluids, of solid microstructures and of granular media, fracture at different scales, modelling of living structures, of composite media and of metamaterials, leading to new optical or acoustical properties. The editors are grateful to participants who accepted to make a written contribution after the Conference. When not available, the text of lectures is replaced by the Abstract. The next Symposium, CMDS 12, is planned to take place in India during winter 2010-2011.

Acknowledgments

The Symposium was successful thanks to the efficient work of the Local Organising Committee (Ecole des Mines de Paris, France): Dominique Jeulin (Chairman CMDS 11), Samuel Forest, Danièle Gozlan and Catherine Moysan. We are grateful to “Centre de Morphologie Mathématique”, and to “Fondation des Industries Minérales, Minières et Métallurgiques Françaises à l’Ecole des Mines de Paris” (FIMMM) for their help to organise CMDS 11. It would have been extremely difficult to have CMDS 11 in Paris without the hospitality of Ecole des Mines de Paris.

We acknowledge the Commissariat à l’Energie Atomique (CEA) for his financial support.

Finally, we are indebted to Silvia Dekorsy and to “Presses de l’Ecole des Mines de Paris” for accepting to publish these Proceedings.

Dominique Jeulin
Chairman of CMDS 11
Fontainebleau, March 4th 2008

Part I

Thermodynamics, transport theory and statistical mechanics in the context of continuum modeling of discrete systems

DUALITY IN ONE DIMENSIONAL TRANSPORT: BOUNDARY LAYER APPROACH

Somendra M. Bhattacharjee¹

¹ Institute of Physics, Bhubaneswar-751005, India
somen@iopb.res.in

ABSTRACT: We discuss the duality between the bulk phase transition and a boundary transition in nonequilibrium asymmetric exclusion process. By using a continuum description, it is shown that the bulk phase transitions can be understood as a deconfinement of a boundary layer, to be called the shockening transition. The duality gives the nature of the phase diagram and the exponents, especially near critical points for shock formation. This is also applied in an interacting model to study the nature of a nonequilibrium tricritical point.

Keywords: Nonequilibrium phase transitions, duality, tricriticality

1 INTRODUCTION

Our purpose in this paper is to show that boundary layers can be used to understand both qualitatively and quantitatively the bulk phase transitions in steady states of a class of nonequilibrium systems. The systems we have in mind are the well-studied asymmetric exclusion process (ASEP) with interacting particles.

The problem with nonequilibrium system is the absence of any hamiltonian. An associated problem is the definition of conjugate variables, because such pairs in equilibrium (analogs of pressure - volume type pairs) are defined via derivatives of the free energy. Nonetheless, the steady states are close cousins of the equilibrium states. The nature of the steady states can be changed by tuning the parameters of the system and this leads to the possibility of nonequilibrium phase transitions. The resulting phases can be represented in a phase diagram in the relevant parameter space. An important feature is that the bulk phase transitions are boundary driven - a phenomenon not found in equilibrium in general.

Bulk phase transitions involve large length scales and only certain gross features of the models are expected to matter at these length scales. Consequently a continuum or hydrodynamic description is useful. By this process, one achieves a separation of length scales, that can be exploited to identify the boundary driven phenomena. Since nonequilibrium problems are characterized by the existence of nonvanishing currents in the system, the nature of currents hold vital information about the system.

2 MODEL

In asymmetric exclusion process, particles are injected at $i = 0$ of a lattice at a rate α per unit time and withdrawn at $i = N$ at a rate $1 - \gamma$ per unit time. The lattice spacing a is much smaller than the total length Na ($a \ll Na$). The particles hop unidirectionally to the right only if the next site is unoccupied or empty. This is the hard core repulsion (exclusion) of the particles. The injection and the withdrawal of the particles act as the drive that forces a current from left to right. This hopping process conserves the particle number along the track. In addition to the hopping, one may allow particle exchange with the surrounding. A particle can be absorbed at a site at a rate ω_a if it is vacant while an occupied site may lose a particle (desorption) at a rate ω_d . These

processes do not conserve particle number on the track. In absence of hopping, the evaporation/deposition process would like to maintain an average density at each site without any current along the track. This is therefore an equilibrium like situation (Langmuir kinetics) that tries to maintain a homogeneous density $\omega_a/(\omega_a + \omega_d)$. The competition of the conserved and nonconserved processes leads to inhomogeneity in the density profile and occasionally discontinuities in the density ("shocks").

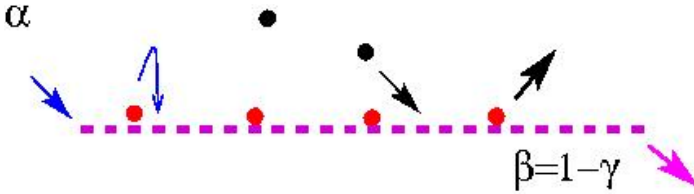


Figure 1: The model:

The possible steady states are shown in the phase diagram of the two external parameters α and γ in Fig. 2. In the low α region, the bulk density profile is determined by the injection rate and is to be called the α -phase (also called the low density phase) while for large α , the bulk density is controlled by the withdrawal rate. This phase is to be called the γ -phase. Inbetween there is a phase where the injection rate and the withdrawal rates control their own territories, meeting at a point with a discontinuity (or a "shock"). This phase is the shock phase.

The phase diagram for the conserved case shows three phases, the α -, the γ - and a maximal current phase (a dream of any traffic engineer). Nonconservation not only kills this maximal current phase but instead introduces a shock phase (traffic jam - a nightmare).

We adopt an equilibrium like definition that if the density shows a jump in going from one phase to the other, it is a first order transition, but if it changes continuously then it is a continuous or critical transition. The α - to the shock phase transition is first order because the shock height is finite on the phase boundary. However, the shock height vanishes at a particular point (α_c, γ_c) . If α is changed at a fixed $\gamma = \gamma_c$, then on crossing the phase boundary, the shock height increases from zero as one enters the shock phase. This, by definition, is a critical point which does not occur in the conserved case. For $\gamma < \gamma_c$, the phase boundary is accidentally a continuation of the critical point. The shock to the γ -phase is also first order without any critical point. In this paper we concentrate on the phase boundary for the α -phase to the shock phase, especially in the neighbourhood of the critical point.

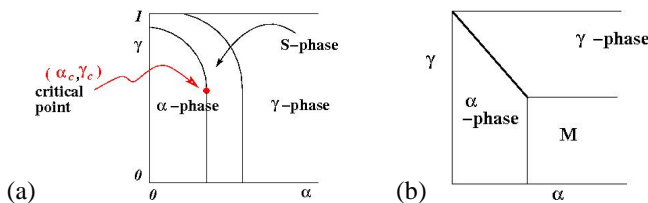


Figure 2: The phase diagrams for the nonconserved (a) and the conserved (b) model.

The density profiles in the three phases of the nonconserved case are shown schematically in Fig. 3. The point to note in these diagrams is the behaviour near the boundary. These are the boundary layers on which we would focus in this paper.

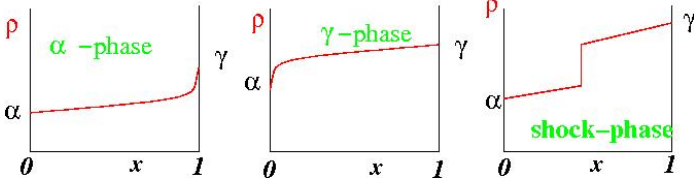


Figure 3: The density profile for the three phases of the nonconserved case.

2.1 Exponents

The critical point has a few characteristic exponents. E.g.,

- The shape of the phase boundary near the critical point is given by

$$|\gamma - \gamma_c| \sim |\alpha - \alpha_c|^\chi. \quad (1)$$

- The shock height h goes to zero along the phase boundary as

$$h \sim s^\beta, \quad (2)$$

where s measures the deviation from the critical point along the phase boundary. For the type of phase boundary shown in Fig. 2a, s can be taken as $\Delta\gamma \equiv \gamma - \gamma_c$.

- In the shock phase the location of the shock is in the bulk of the system. As one approaches the phase boundary within the shock phase, the location x_s of the shock should approach the boundary $x = 1$, as

$$1 - x_s \sim |\alpha - \alpha_c|^\zeta. \quad (3)$$

- Within the shock phase if one approaches the critical point along $\gamma = \gamma_c$, the shock height vanishes as

$$h \sim |\alpha - \alpha_c|^{\bar{\beta}}. \quad (4)$$

These exponents are determined by the boundary behaviour and the boundary layer itself is characterized by two exponents, one describing its intrinsic width w and the other one its location ξ from the boundary. The location ξ is a measure of the thickness of the layer. The width w diverges at the critical point but the thickness ξ diverges as the shock is formed from the α -phase or the γ -phase side. The divergence of ξ is associated with the “shockening” transition to be explained below. The exponents describing these boundary effects are

$$\xi \sim |\alpha - \alpha_s|^{-\zeta_-}, \quad \text{for } \alpha \rightarrow \alpha(\gamma)_-, \gamma \neq \gamma_c \quad (5)$$

$$w \sim |\alpha - \alpha_c|^{-\zeta_c}, \quad \text{for } \alpha \rightarrow \alpha_c - \text{ with } \gamma = \gamma_c. \quad (6)$$

Note that the boundary characteristic exponent ζ_- is the analog of the bulk exponent ζ of Eq. (3).

Since the bulk and the boundary transitions are linked, one needs exponents that couple them. One of these is the relation between w and h . On the first phase boundary,

$$w \sim h^{-\eta}, \quad (7)$$

which connects the divergence of w at the critical point with the vanishing of the shock height.

3 DESCRIPTION

The microscopic variables are the occupation numbers $t_i = 0, 1$ of the i th site with 0 denoting unoccupied and 1 denoting occupied sites. In a coarse grained description and in the continuum limit, we replace these microscopic variable by the average occupation number or density $\rho(x)$ where $x = i/N$ is the position variable in the range $[0, 1]$. This continuum limit is valid for $Na \gg a$ (a being the lattice spacing). In our approach $\epsilon = 1/N$ is a small parameter. In the steady state the spatially average density is

$$M = \int_0^1 \rho(x) dx \quad (8)$$

This can be used to define response functions that monitor sensitivity to the external drives, namely,

$$\chi_\mu = \frac{\partial M}{\partial \mu}, \quad \mu = \alpha \text{ or } \gamma. \quad (9)$$

For example, for the α -phase, $\chi_\alpha \sim O(1)$ but $\chi_\gamma = 0$. Both are nonzero for the shock phase. Thus χ_μ can be used to identify phases.

In the continuum limit, the variation of the density can be written as a modified continuity equation,

$$\frac{\partial \rho(x)}{\partial t} + \frac{\partial J_0(x, t)}{\partial x} = S_0(\rho, t), \quad (10)$$

where $J_0(x, t)$ is the current through the track and S_0 is the nonconserved current. For the simple uncorrelated Langmuir dynamics we are considering,

$$S_0 = \Omega(\rho_L - \rho), \quad \text{where } \rho_L = \frac{\omega_a}{\omega_a + \omega_d}, \quad \Omega = N(\omega_a + \omega_d). \quad (11)$$

The nonconserved processes matter if the total flux Ω is comparable to the current and so Ω is taken to be $O(1)$ in the limit $N \rightarrow \infty$. We take $\rho_L \neq 1/2$ or $\omega_a \neq \omega_d$.

The current in the mean field approximation is taken to be determined by the local density so that it can be written as

$$J_0 = -\epsilon \frac{\partial \rho}{\partial x} + j(\rho(x, t)), \quad (12)$$

where j is the bulk current. There is an extra term reminiscent of Fick's law but with vanishingly small diffusion constant $\epsilon = 1/N$. This small diffusion constant plays an important role in determining the phase transitions. The form of $j(\rho)$ is known for several cases. In case there is a particle-hole symmetry, the simplest form is $j = \rho(1 - \rho)$. A double-peaked current density is also known to occur in an interacting system. With the form of current in Eq. 12, the equation governing the density is of the form

$$-\epsilon \frac{d^2 \rho}{dx^2} + S_1(\rho) \frac{d\rho}{dx} + S_0(\rho) = 0, \quad \text{where } S_1(\rho) = \frac{dj(\rho)}{d\rho}. \quad (13)$$

A simple expression like $j(\rho) = \rho(1 - \rho)$ quite often helps to check the general results and suffices for the simple ASEP model we have defined. More complicated form will be introduced below. $S_1(\rho)$ is zero at the peak of the current, or the density at which current is maximum.

Eq. 13 entails two length scales, (i) x for the bulk and (ii) $\tilde{x} = (x - x_0)/\epsilon$ which is significant only in a thin region as $\epsilon \rightarrow 0$ around an appropriately chosen x_0 . Eq.

13 does not depend on the choice of x_0 . The separation of the two scales is used to develop a uniform approximation of the solution order by order in ϵ . Here we restrict ourselves to the lowest order approximant.

The bulk solution in terms of x comes from the first order equation obtained with $\epsilon = 0$ in Eq. 13. This solution, to be called the outer solution,

$$\rho(x) = \rho_{\text{out}}(x) \quad (14)$$

is given implicitly by

$$g(\rho) = 2\Omega x + C, \quad (15)$$

where C is a constant to be fixed by only one of the two boundary conditions. For the left boundary condition, the outer solution is

$$g(\rho) = 2\Omega x + g(\alpha), \quad (16)$$

with a density

$$\rho_o \equiv \rho_{\text{out}}(1) \text{ at } x = 1, \quad (17)$$

determined by

$$g(\rho_o) = 2\Omega + g(\alpha). \quad (18)$$

In general $\rho_o \neq \gamma$. To satisfy this other boundary condition $\rho = \gamma$ at $x = 1$, we use the second scale $\tilde{x} = (x - 1)/\epsilon$ around the boundary point $x = 1$. With this variable, the density (to be called the inner solution) satisfies

$$-\frac{d^2 \rho_{\text{in}}}{d\tilde{x}^2} + S_1(\rho_{\text{in}}) \frac{d\rho_{\text{in}}}{d\tilde{x}} = 0, \quad (19)$$

obtained from Eq. (9) by first changing the variable to \tilde{x} and then taking $\epsilon \rightarrow 0$. The absence of the S_0 term can be understood from the observation that for a constant Ω this layer is too thin for the nonconservation to matter, at least to leading order in ϵ . For a smooth density profile (the solution of the second order equation), we need to match the outer and the inner solutions by requiring that

$$\lim_{x \rightarrow 1} \rho_{\text{out}}(x) = \lim_{\tilde{x} \rightarrow -\infty} \rho_{\text{in}}(\tilde{x}). \quad (20)$$

Here $\tilde{x} \rightarrow -\infty$ gives the outer limit of the inner solution. Incorporating this matching condition, Eq. 19 can be written as

$$\frac{d\rho_{\text{in}}}{d\tilde{x}} = j(\rho_{\text{in}}) - j(\rho_o), \quad (21)$$

in the thin boundary layer, with $\rho_{\text{in}}(\tilde{x} = 0) = \gamma$. The complete matched solution is obtained by joining the inner and outer approximations and subtracting their common value. Therefore, the density profile is given by

$$\rho(x) = \rho_{\text{out}}(x) - \rho_o + \rho_{\text{in}}(\tilde{x}) + O(\epsilon). \quad (22)$$

Eq. 22 identifies the scale dependent separation of the bulk and the boundary contributions and it provides a uniform approximation of the density in the whole domain including the boundaries.

3.1 Shocks from Boundary layers: Shockening transition

A shock is formed if the inner solution fails to satisfy the boundary condition $\rho(x=1) = \gamma$. If the inner solution saturates to a density ρ_s as $\tilde{x} \rightarrow \infty$ then Eq.21 can also be written as

$$\frac{d\rho_{\text{in}}}{d\tilde{x}} = -(\rho - \rho_o)(\rho - \rho_s)\Phi(\rho) \quad (23)$$

where one zero of the function at ρ_o corresponds to the matching condition and the other one for the saturation. The inner solution is of the form

$$\rho_{\text{in}}(\tilde{x}) = \mathcal{I}(\tilde{x}/w + \xi) \text{ with } \mathcal{I}(z) \rightarrow \rho_s \text{ or } \rho_o \text{ as } z \rightarrow \pm\infty. \quad (24)$$

Here w is the width of the layer and ξ gives the location of the center of the layer - the two quantities defined in Eqs. (5) and 6. Even if ξ is outside the physical range it helps in visualization of the shock formation. This form gives a direct interpretation of the width w but one may also define w from the approach of the inner density to the bulk asymptote in the outer region.

There are two types of solutions for the inner density(4), one bounded between ρ_o and ρ_s while the other one shows a divergence with $d\rho/dx \sim -\rho^2$, or more generally, $d\rho/dx \sim -\rho^{2p}$. It transpires that for the class of unbounded solution it is always possible to match the boundary condition by suitably shifting the center of the inner solution. This will not be the case for the bounded solution. The significance of this is that the bounded solution can give rise to shocks but not the unbounded ones.

For a given α , as γ is changed, two different situations may arise; the origin or the center of the layer shifts either to $-\infty$ ($\xi \rightarrow -\infty$) or to $+\infty$, $\xi \rightarrow +\infty$.

In the first situation, the boundary layer as seen in the physical range thickens but remaining pinned to the boundary. As $\xi \rightarrow -\infty$ (note this is the inner scale), the layer gets released from the boundary and moves into the bulk. The transition of a thin layer to a shock at $\gamma = \rho_s(\alpha)$ has been called a ‘‘shockening’’ transition(3). So long as the boundary layer stays pinned to the boundary, $\chi_\gamma \sim \epsilon\gamma/\hat{S}_1(\gamma) \rightarrow 0$ as $\epsilon \rightarrow 0$. In contrast, χ_α is nonzero. The phase, by definition, is then an α -phase. The bulk shock phase boundary is given by $\gamma = \rho_s(\alpha)$.

The occurrence of the two zeros of $\hat{S}_1(\rho)$ in Eq. 23 suggests that there has to be another line $\gamma = \rho_o(\alpha)$ at which $\xi \rightarrow +\infty$. We call this the Mukherji-Mishra (MM) dual boundary line because a similar feature was observed in Ref. (4). As one crosses this MM line the boundary region goes from an accumulated to a depleted region, thereby separating the shockening to nonshockening boundary layers. This MM dual line is purely a boundary transition line, and its existence is a requirement for shock formation at $\gamma = \rho_s(\alpha)$. Since (ρ_o, ρ_s) need to occur in pair, we call the $\gamma = \rho_o(\alpha)$ as the dual line of the bulk phase boundary.

Once we know the bulk phase boundary and the dual line, we can obtain the width of the layer. From the asymptotic approach to the limits ρ_o and ρ_s , one gets from Eq. 23, $w^{-1} = (\rho_s - \rho_o)\Phi(\rho_X)$ with X denoting ‘o’ or ‘s’. This also shows the possibility of a critical point where w diverges. It happens if the shockening transition line and the dual line intersect. The intersection is at $\gamma = \gamma_c$ and since $\rho_o \rightarrow \rho_s$, we find $w \rightarrow \infty$, with $\eta = 1$ (see Eq. 7). It also follows that the shock height remains nonzero at the bulk phase transition from the α -phase to the shock phase. On the other hand, the shock evolves from a zero height at the crossing point so that it is a continuous transition. In case the two lines do not cross, there will be no critical point and the lines will be symmetrically placed around $\gamma = \rho_m$, the maximum current density. The bulk phase diagram corresponds to Fig. 2.

The exponents follow from the analytical behaviour of the outer solutions $g(\rho)$. Noting that $dg(\rho)/d\rho = 0$ at $\rho = \rho_c$, one gets

$$\zeta_c = 1/2, \zeta_- = 0(\log), \text{ and } \eta = 1, \quad (25)$$

where for completeness we have included η obtained above. The notation ‘‘(log)’’ means a logarithmic divergence because the power law exponent is zero.